Pepticinnamins N, O and P, cytotoxic non-ribosomal peptides from a Soil-Derived *Streptomyces mirabilis* P8-A2

Manar M. Mahmoud,[1] Maria Mahmoud Abboud,[1] Matiss Maleckis,[2] Luciano D. O. Souza,[3,4] José M. A. Moreira,[4] Charlotte H. Gotfredsen,[5] Tilmann Weber,[2,*] Ling Ding[1,*]

[1] Department of Biotechnology and Biomedicine, Technical University of Denmark, Søltofts Plads 221, 2800 Kgs. Lyngby, Denmark.

[2] The Novo Nordisk Foundation Center for Biosustainability, Technical University of Denmark, Søltofts Plads, Building 220, 2800 Kgs. Lyngby, Denmark.

[3] Sino-Danish Center for Education and Research, Denmark; Department of Drug Design and Pharmacology, University of Copenhagen, Denmark

[4] Department of Drug Design and Pharmacology, University of Copenhagen, Denmark

[5] Department of Chemistry, Technical University of Denmark, Kemitorvet Building 207, 2800 Kgs. Lyngby, Denmark.

[*] Corresponding authors: Ling Ding, Phone: 0045-50333791, email: lidi@dtu.dk; Tilmann Weber, Phone: 0045-24896132; email: tiwe@biosustain.dtu.dk

Cinnamoyl moiety containing non-ribosomal peptides represented by pepticinnamin E, are a growing family of natural products isolated from different *Streptomyces* and possess diverse bioactivities. A soil bacterium *Streptomyces mirabilis* P8-A2 harbors a cryptic pepticinnamin biosynthetic gene cluster, producing azodyrecins as major products. Inactivation of the azodyrecin biosynthetic gene cluster by CRISPR-BEST base editing led to the activation and production of pepticinnamin E (**1**) and its analogues, pepticinnamins N, O and P (**2-4**), the structures of which were determined by detailed NMR spectroscopy, HRMS data, and Marfey´s reactions. These new compounds exerted modest growth inhibitory effect against the LNCaP and C4-2B prostate cancer lines, respectively, with pepticinnamin O being the most active.

Despite the genetic diversity indicated by diverse genome mining tools, 70% of the secondary metabolites from *Streptomyces* remain unknown since most corresponding genes are normally "cryptic" in standard laboratory culture conditions.[1–4] To activate the production of these compounds many approaches can be taken, especially using synthetic biology and ecological approaches.[5,6] Examples are genetic manipulation,[7] heterologous expression of a biosynthetic gene cluster (BGC) in another host,[8] and co-cultivation,[9] which can unravel the potential of metabolite production and allow for "silent" gene activation, allowing for a vast number of potentially valuable compounds to be discovered.

Non-ribosomal peptides (NRPs) such as the antibiotic vancomycin are an important group of secondary metabolites synthesized by Non-Ribosomal Peptide Synthetases (NRPSs). Among them, cinnamoyl moiety containing NRPs are a small family of natural products isolated from different *Streptomyces* and possess diverse bioactivities. Examples are atratumycins[10] and atrovimycin[11] active against *Mycobacterium tuberculosis*, mohangamides A with inhibitory activity against *Candida albicans* isocitrate lyase,[12] WS9326A-E, inhibiting *Brugia malayi* asparaginyl-tRNA synthetase,[13] and coprisamides A and B with activity for induction of quinone reductase.[14]

Pepticinnamins represent a growing class of interesting group of NRPs, showing various activities. For example, pepticinnamin E is active as a farnesyl transferase inhibitor,[15] and RP-1776 is inhibiting the binding of the platelet-derived growth factor with two B subunits (PDGF-BB) to the PDGF beta-receptor.[16] Two pepticinnamin BGCs, *pcm* and *pep*, have recently been described,[17,18] encoding pepticinamins G-M, new analogues of pepticinnamin E.

S. mirabilis P8-A2 is a soil *Streptomyces*, a producer of a novel group of rare cytotoxic azoxyl metabolites, azodyrecins.[19] Genome-mining using antiSMASH[20] revealed a BGC with close to identical similarity score, 96%, to *pep* BGC of *S. mirabilis* OK006 (published under name *Actinobacteria bacterium* OK006).[17] However, the BGC remained silent since we could not detect pepticinnamins through LC-MS profiling under all conditions tested. Interestingly, during the investigation of the biosynthesis of azodyrecins, the inactivation of *azdB*, a core gene in the azodyrecin biosynthesis[21], led to a higher production of several pepticinnamins including the previous reported pepticinnamin E and several new analogues.

In this study we report the structure elucidation of three novel analogues of pepticinnamins, N, O and P, their biological activities, and comparison of pepticinnamin biosynthetic gene clusters.

RESULTS AND DISCUSSION

Activation of pepticinnamin BGC

S. mirabilis P8-A2 produces azodyrecins as major metabolites. While investigating the biosynthesis of azodyrecins, we inactivated *azdB*, which catalyzes the formation of the azo-moiety in azodyrecin biosynthesis[21]. In addition to the accumulation of azodyrecin-precursors, we also identified the production of several unrelated compounds, identified as pepticinnamins, including the previous reported pepticinnamin E (**1**) (**Figures 1-2**) and several new analogues (**2-4**) (**Figures 1-2**). Obviously, the inactivation of the azodyrecin BGC impacted the specialized metabolite regulatory networks or diverted the metabolism flux toward pepticinnamin production. All four peaks displayed similar UV profiles with a maximum absorption at 225 and 282 nm, respectively. Dereplication through Reaxys[22] and The Natural Product Altlas[23] indicated the production of pepticinnamin E (**1**) with a formula of $C_{49}H_{54}ClN_5O_{10}$ together with the other three new analogues (**2-4**) with the formula of $C_{49}H_{55}N_5O_{10}$, $C_{44}H_{48}ClN_3O_8$ and $C_{44}H_{49}N_3O_8$. Further MS/MS fragmentation (Figure S32-35) confirmed that they are new analogues of pepticinnamin E.

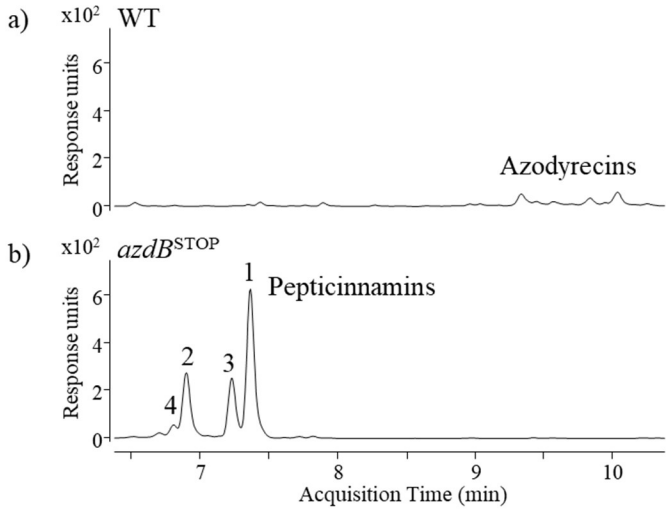

Figure 1. LC/MS profile showing the activation and production of pepticinnamins in *S. mirabilis* P8-A2. a) wild type (WT) showing the production of azodyrecins at the retention time of 9.2-10.8 min, b) azdB^{STOP} mutant led to production of pepticinnamins (**1-4**) (*m/z* $[M + H]^+$ 909.3651, 874.4017, 782.3216, and 748.3599) at the retention time of 7.4, 6.9, 7.2,and 6.8 min respectively.

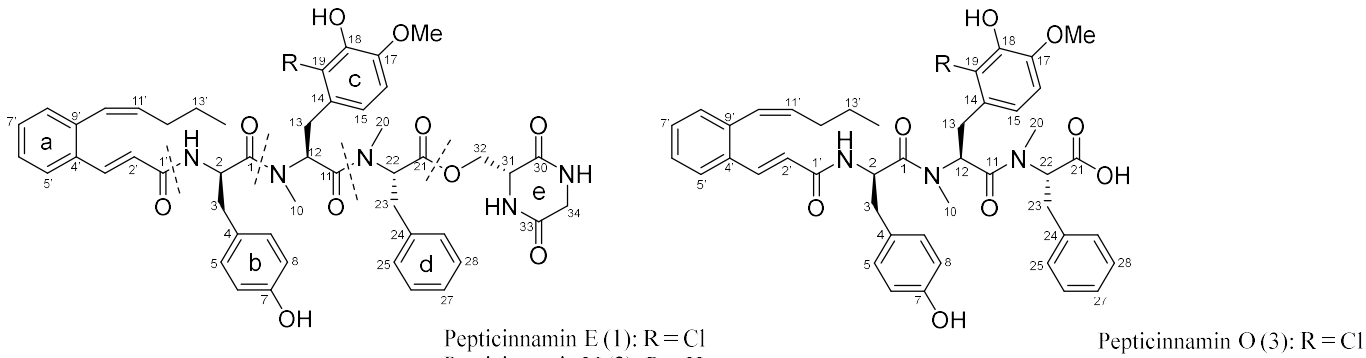

Figure 2. The structures of pepticinnamins (**1–4**) discovered from the *S. mirabilis* P8-A2 *azdB* Q73* mutant.

Isolation and characterization of pepticinnamins

To obtain enough materials and confirm the chemical structures for the new pepticinnamins, we have scaled up the fermentation of the mutant *S. mirabilis* P8-A2 (*azdB*^{STOP}) [21] through a 5 L solid fermentation using soya flour mannitol (SFM) agar plates for 10 days to yield a 7.2 g of EtOAc crude extract, which was subjected to a flash column chromatography on C-18 silica gel, and Sephadex LH-20 followed by further purification using preparative HPLC, yielding compounds **1** (5 mg), **2** (2 mg), **3** (2.5 mg) and **4** (3 mg) which were studied by NMR (Tables 1 and 2), MS, and Marfey´s reaction.

Compound **1** was isolated as a yellowish powder. High-resolution electrospray ionization mass spectrometry (HRESIMS) (Figure S1) revealed a formula of $C_{49}H_{54}ClN_5O_{10}$. The NMR spectrum showed signals for three methyls, a methoxy group, seven methylenes, nineteen methines. Numerous olefinic signals from several spin systems were further confirmed by COSY spectrum. The ^{13}C NMR spectrum showed the presence of six carbonyl signals corresponding to potential ester or amide moieties, which indicated **1** as a peptide. The interconnection between the six building blocks of **1** (a, b, c, d, and e) (**Figure 3**) for **1** was deduced from ^{1}H-H COSY, and HMBC (**Figure 3**). The partial structure a corresponded to the cinnamic acid derivative showing ^{13}C NMR resonances at δ_C 165.9, 140.4, 135.9, 134.4, 131.2, 130.4, 128.4, 128.2, 127.1, 122.5, 31.7, 23.7, 14.2. Chemical shifts in the ^{1}H NMR spectrum revealed a methyl group (δ_H 0.84), two methylene protons (δ_H 2.01, 1.40), four aromatic methines (δ_H 7.66, 7.34, 7.29, 7.22), and two pairs of alkene methines (δ_H 7.77, 6.45 and 6.60, 5.86). The HMBC correlation between H2 δ_H 5.02 and the amide ca**r**bonyl C1' (δ_C 165.9) established the attachment of the cinnamoyl moiety to the residual amino acid tyrosine (b).

The partial structure b showed a typical chemical equivalence between the two methine doublets with 2H integration on the aromatic ring (δ_H 7.04 and 6.73), a methylene (δ_C 38.4, δ_H 2.83, 2.62) group with a ^{3}J correlation

to the amide carbonyl δ_C 171.9 as a part of the peptide linkage to the adjacent amino acid. 2-Chloro-3-hydroxy-4-methoxy-phenylalanine as partial structure c showed two doublets aromatic methines at (δ_H 6.51) indicated by ^{1}H -^{1}H COSY, while in the HMBC spectrum a methoxy group at (δ_H 3.57), methylene protons at (δ_H 3.10, 2.76) exhibited ^3J coupling to the amide carbonyl at δ_C 171.9 (**Figure**). Additionally, the *N*-methyl proton (δ_H 2.30) of partial structure d correlated to the C11 amide carbonyl indicated by the downfield shift δ_C 171.9 of the N-methyl-phenylalanine amino acid moiety. Finally, the positions of different peptide bonds were confirmed by key HMBC correlations. The methylene protons (δ_H 4.56 and 4.41) showed HMBC correlations with the ester linkage C21 (δ_C 171.2) confirmed the serine-glycine diketopiperazine residue (partial structure e); HMBC correlations of the CH_2 protons (δ_H 4.04 and 3.92) of glycine with the carbonyl C-30 (δ 167.7) of serine; and the HMBC correlations of the C-32 methylene protons (δ_H 4.56 and 4.41) of serine with the carbonyl C-33 (δ 168.5) of glycine, alongside the MS/MS fragmentation pattern (Figure S32) confirming the structure of **1** as pepticinnamin E. Elucidation of the absolute configuration was carried out by Marfey´s reaction and is described in the following section.

Compound **2** was obtained as a colorless solid. HRESIMS (Figure S2) analysis revealed a formula of $C_{49}H_{55}N_5O_{10}$, as a new analogue of pepticinnamin E with a loss of a chloride atom compared to pepticinnamin E. Indeed, **2** exhibited a similar ^{1}H NMR spectrum, except the appearance of one additional aromatic proton at δ_H 6.73 (H-19). In the ^{13}C NMR spectrum, the chemical shift for C-19 appeared upfield (δ_C 116.3) compared to pepticinnamin E (δ_C 122.1). In addition, the position for the three aromatic protons was further confirmed by the coupling constant, an *ortho*-coupling $J_{15\text{-}16}$ = 8.3 Hz, and a *meta*-coupling $J_{15\text{-}19}$ = 2.1 Hz, respectively. The above data suggested the lack of chlorine-substitution at C-19. These results were confirmed by COSY, HSQC, H2BC and HMBC experiments (**Figure**). Thus, compound **2** was identified as previously undescribed pepticinnamin N.

Compound **3** was isolated as a second new analogue, a colourless solid and HRESIMS (Figure S3) analysis confirmed a formula of $C_{44}H_{48}ClN_3O_8$, which indicated a shorter peptide chain compared to pepticinnamin E. MS/MS fragmentation (Figure S34) indicated the loss of the Gly-Ser diketopiperazine moiety. This was further confirmed by ^{1}H NMR and ^{13}C NMR spectra, where signals for the aromatic rings remained conserved, while the signals for the Gly-Ser diketopiperazine moiety disappeared. Compared to pepticinnamin E, the ^{1}H and ^{13}C NMR spectra of compound **4** lacked signals attributed to the diketopiperazine moiety from the cyclization of serine and glycine residues. These data in combination with the COSY, HSQC, H2BC and HMBC experiments (Table 1 and **Figure**) identified pepticinnamin O.

Compound **4** was isolated as an analogue of **3** and HRESIMS (Figure S4) analysis confirmed a formula of $C_{44}H_{49}N_3O_8$ which indicated a loss of one chloride atom compared to pepticinnamin O. This was supported by an additional aromatic proton appearing at δ_H 6.70 in the ^{1}H NMR spectrum the chemical shift of C-19 with δ_C 122.0

in pepticinnamin O was upfield shifted to δ 116.2 (Table 1 and **Figure**). MS/MS fragmentation (Figure S35) indicated a loss of the Gly-Ser diketopiperazine moiety. Thus, compound **4** was identified as a new pepticinnamin analogue named pepticinnamin N.

Pepticinamins were first isolated in 1993 by Ōmura et al.[15] from *Streptomyces* sp. OH-4652 and were found to act as natural protein farnesyltransferase (PFT) inhibitors with relative inhibitory potency (IC_{50}) from 6-fold- to 60-fold higher than that of synthetic peptides.[15] Following these findings and considering the molecular structure of pepticinnamin E, Hinterding et al.[24] took the initiative of determining whether pepticinnamin E acted as a mono- or bisubstrate inhibitor of the PFT enzyme, thereby imitating the farnesyl group, the peptide substrate or both. In their study, Hinterding et al. chemically synthesized both diastereomers of pepticinnamin E, and showed them to actually act as competitive inhibitors with respect to both the peptide substrate (CAAX amino acid sequence of the Ras protein) and FPP.[24] Furthermore, their study showed that terminal modifications (at the C- and N-terminals) to pepticinnamin E are of minor impact for the inhibition of farnesyl transfer and that the central amino acids and their absolute configuration are decisive for pepticinnamins' inhibitory activity.[24] In the study by Ge et al., pepticinnamin G, which only differed from pepticinnamin E in the configuration of its first amino acid (L-tyrosine) and the type of its third amino acid (*N*-methyl-L-alanine), was tested for its biological activity in human cancer cell lines sensitive to Ras PFT inhibitors.[18] The experiment showed no growth inhibition against these cancer cell lines at 10 μM.[18,24] These results further confirmed the findings of Hinterding et al. on the decisiveness of the central amino acids and their absolute configuration on pepticinnamins' inhibitory activity.[18,24] With pepticinnamins displaying a high degree of selectivity for the PFT enzyme and being the only naturally produced bisubstrate inhibitors of PFT, the structure of pepticinnamin E became a starting point for investigating additional anchor points that could be exploited to design more potent and selective antagonists.[25] Furthermore, the demands for bisubstrate PFT inhibitors has driven Prof. Waldmann and a number of other research groups to initiate the synthesis of pepticinnamin E analogue libraries that could potentially meet these demands.[25–28]

In the study by Omura et al.,[15] it was found that pepticinnamin E showed no antimicrobial activity at a concentration of 1,000 μg/ml against various test microorganisms. The antimicrobial activity of compounds **1–4** was evaluated against the bacteria *Staphylococcus aureus* 8325, *Bacillus subtilis* and *Pseudomonas aeruginosa* PAO1 and yeast *Candida albicans* IBT 656 using a standard broth microdilution method. No antimicrobial activities were observed (MIC >50 μg/mL).

RAS proteins are frequently mutated or dysregulated in various human solid tumors, and aberrant expression and activation of RAS proteins has been implicated in oncogenesis, tumor-cell invasion and metastasis. RAS function is dependent on its association with the cell membrane, which in turn requires a series of post-translational

modifications, first and foremost attachment of a farnesyl isoprenoid by farnesyltransferase.[29] As a result, natural inhibitors of FTase are potential anti-RAS drugs and, as such, have been considered interesting compounds for cancer treatment. We tested the effect of pepticinnamins E, O, and N on cell viability and proliferation of the LNCaP and C4-2B human epithelial prostate cancer cell lines (**Figure 4**). Cells were grown in the presence of 10μM pepticinnamin E, O, or N for 72h. We found that only pepticinnamin O exhibited growth-inhibitory effects at this concentration, of 12.1% and 11.3% in LNCaP and C4-2B, respectively. Pepticinnamins E and N showed no significant effects on growth rates of LNCaP or C4-2B cells. Pepticinnamins E or N also had no significant cytotoxicity in LNCaP or C4-2B cells under the tested conditions - 10μM concentration and 72h exposure. Exposure to pepticinnamin O caused a small decrease in cell viability (15.3%) in LNCaP cells but had no significant effect on C4-2B cells. We also evaluated the effect of pepticinnamin O on the multi-drug resistant sublines LNCaP^{R} and C4-2B^{R}, which overexpress the drug efflux pump P-glycoprotein (Pgp), and found it to exert cell growth inhibition in these cells, 25.7% and 12.8% in LNCaP^{R} and C4-2B^{R}, respectively, suggesting it can evade Pgp-mediated multidrug resistance.

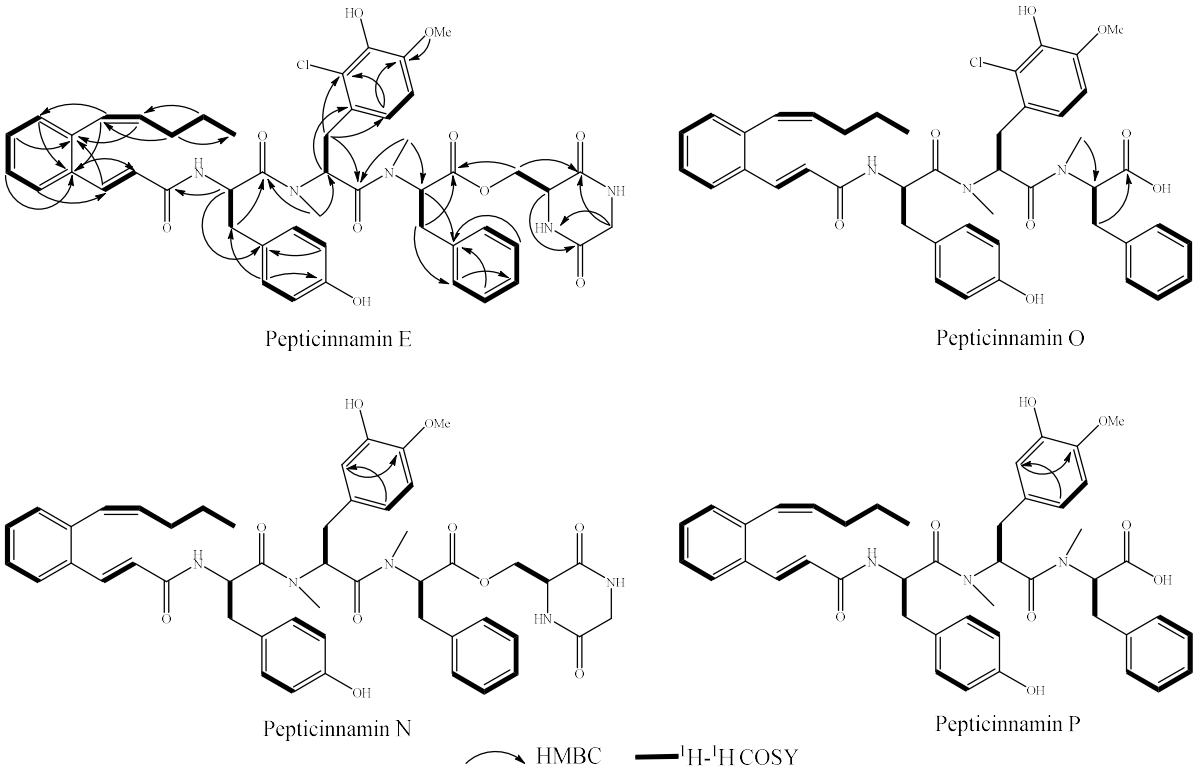

Figure 3. COSY and HMBC correlations of pepticinnamin E (**1**) and its three new analogues (**2–4**).

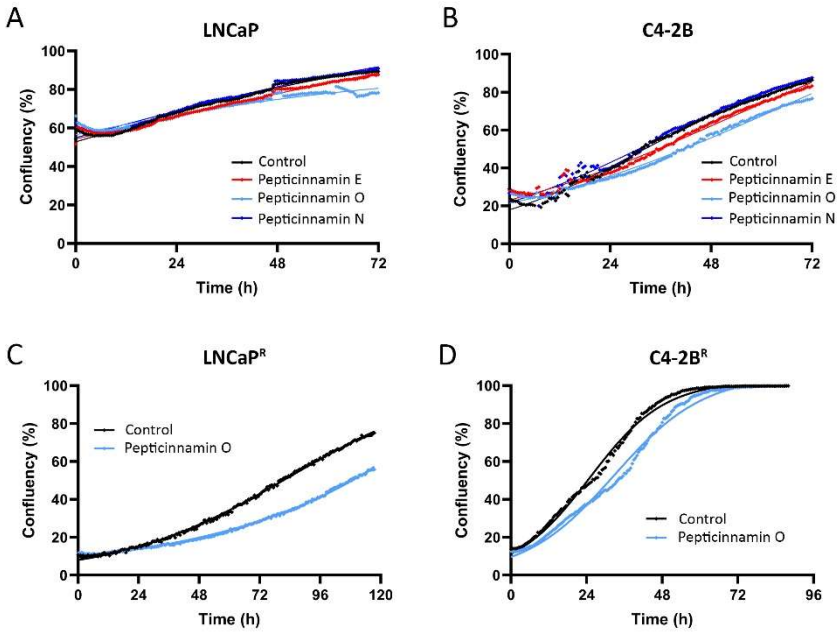

Figure 4. Pepticinnamins effect on cell growth. Label-free confluence measurements of (A) LNCaP, (B) C4-2B, (C) LNCaP^R, and (D) C4-2B^R prostate cancer cells, grown in the presence of 10 µM pepticinnamin E (red line), O (cyan line), or N (blue line), or control (vehicle, black line), respectively, showed only modest growth-inhibitory effects for pepticinnamin O. Representative experiments are presented.

Chirality elucidation through Marfey´s reaction

For pepticinnamin E, Õmura et al. detected the stereochemistry of three chiral centers, D-tyrosine, *N*-methyl-L-phenylalanine and D-serine, however they left the fourth, corresponding to the DOPA derivative, undefined due to its decomposition during purification.[30] The configuration of the DOPA derivative remained undefined until 1998, when Hinterding et al. performed a total synthesis of pepticinnamin E and its epimer thereby showing the second amino acid to possess an L-configuration after experimentally comparing the two epimers with the natural pepticinnamin E.[15] In another study in 2020 by Ge et al., the marine *Streptomyces* sp. PKU-MA01144 was found to naturally produce three new analogues of pepticinnamin E, namely pepticinnamins G-I, and four other analogues, namely pepticinnamins J-M, from several constructed mutants of the natural producer.[18] All possess an L-tyrosine configuration instead of a D-tyrosine configuration and an *N*-methyl-L-alanine amino acid instead of an *N*-methyl-L-phenylalanine, which are the two main structural features that distinct this group of analogues from pepticinnamin E (**Figure 5**).[18] In the current study the Marfey´s analysis method was used to conduct the absolute configuration of compound **1.**

As a result, LC-MS analysis of the derivatives showed the same retention time as those prepared from a sample of authentic standards previously reported in the literature[18] as D-tyrosine, *N*-methyl-L-phenylalanine, and D-serine.

A D- configuration of *N*-methyl-2-chloro-3-hydroxy-4-methoxy-phenylalanine residue was established by measuring its specific optical rotation ($[\alpha]_D^{25}$ 0.0928, *c* 0.023, MeOH) after purification from acid hydrolysis. This confirmed the absolute configurations of pepticinnamin E. Based on the common biosynthetic pathway, the absolute configurations of **2–4** were established as the same as those of pepticinnamin E. Indeed, they have exhibited similarities in the ECD spectra (Figure S31).

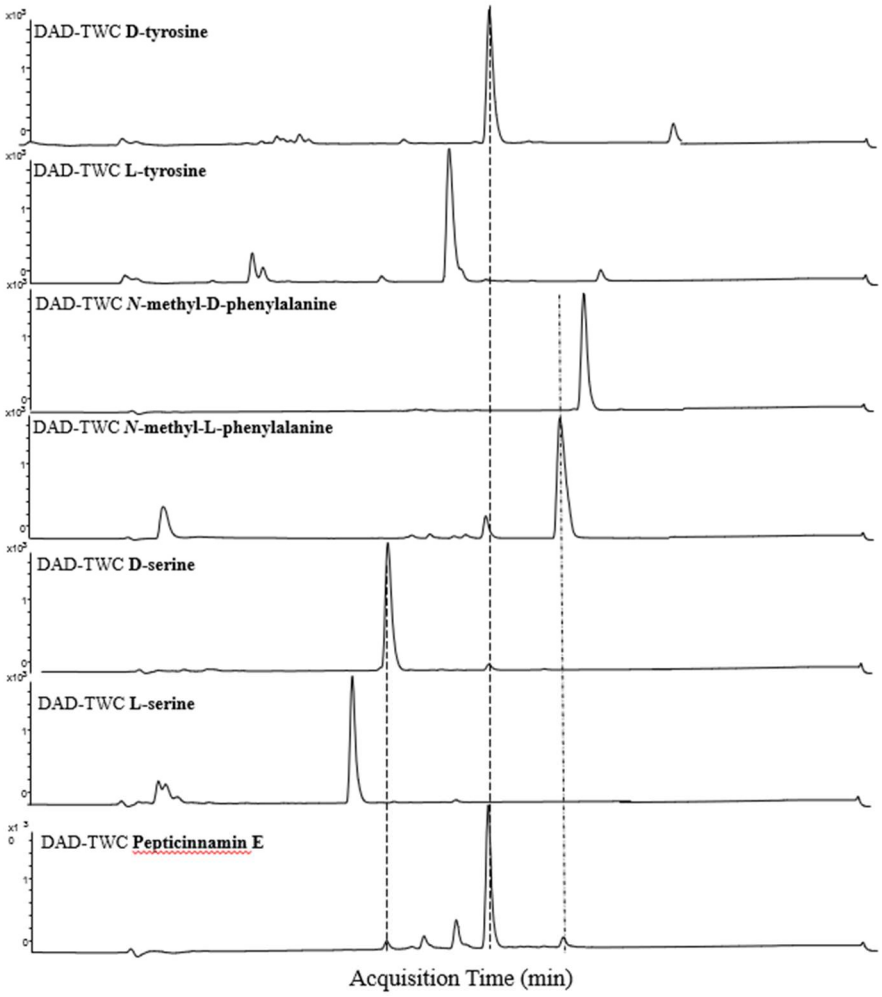

Figure 5. HPLC analysis of the hydrolysates of pepticinnamin E in comparison with standards.

Biosynthesis of pepticinnamins

Although pepticinnamin E has been discovered 30 years ago, the *pcm* BGC has only been described recently in two different producers, *S. mirablilis* OK006 and *Streptomyces* sp. PKU-MA01144, in 2019 and 2020, respectively, through key gene disruption[17] and heterologous expression.[18] The two microorganisms while encoding closely

similar BGC, produces new types of pepticinnamins, pepticinnamins G−I, with difference in chirality of first NRPS amino acid, L- instead of D-tyrosine, and *N*-methyl-L-alanine instead of *N*-methyl-L-phenylalanine.

In 2019,[17] Santa Maria et al. took advantage of the presence of the *N*-terminal cinnamoyl moiety of pepticinnamin E in other natural products with characterized BGCs, such as skyllamycin A. By using Sky28, an enzyme responsible for the formation of the benzene ring in the cinnamoyl moiety of skyllamycin A as a biosynthetic "probe", the pepticinnamin E biosynthetic gene cluster (*pcm* BGC) was discovered in *S. mirabilis* OK006 with estimated size of 45 kbp.[17] The *pcm* biosynthetic gene cluster consisted of two NRPSs, Pcm2 and Pcm30.[17] The entire NRPS consisted of five modules, which is consistent with the uptake of five amino acid residues composing pepticinnamin E. The modular architecture of NRPS domains suggested that the biosynthesis uses L-amino acids, however this was not the case for pepticinnamin E, as they were composed of D-tyrosine and D-serine.[17]

In the study by Ge et al. in 2020,[18] the new pepticinnamin analogues, pepticinnamins G-M,[18] were discovered and isolated from the marine *Streptomyces* sp. PKU-MA01144. They confirmed the biosynthetic gene cluster responsible for production of these pepticinnamins, *pep*, through heterologous cloning, knock out studies and feeding experiments. There are two important differences between the two BGCs. Firstly, the pepticinnamins encoded by *pep* BGC contained an L-tyrosine residue compared to a D-tyrosine in *pcm* BGC. Secondly, the two strains are significantly different, sharing whole genome average nucleotide identity of only 81 %.

The pepticinnamin BGC from *S. mirabilis* P8-A2 is close to identical to the *pcm* BGC of *S. mirabilis* OK006, share 99.1% nucleotide identity and average protein identity of 98%. As expected, the *S.* sp. PKU-MA01144 *pep* BGC is significantly different, sharing 64.3% nucleotide identity and protein identities between 45% and 91%. The differences between *pcm* and *pep* BGC likely explain the differences in chirality of two BGC products. We performed BGC alignment to highlight similarities in the architecture and sequence similarity between the three BGCs using clinker[31] and antiSMASH[20] (**Figure 6**). The *pcm* BGC was earlier analyzed by Santa Maria et al. for presence of NRPS domains that might accept D-tyrosine or have epimerase activity, however bioinformatic analysis indicated L-tyrosine. We came to the same conclusion after comparative genomics and analysis of NRPS domains using the latest antiSMASH 7.0[20] HMMER models, all indicating that L-amino acid is used. The D-tyrosine and D-serine in pepticinnamin E biosynthesis remains a mystery.

Within the NRPS, there are two *N*-methyltransferases domains which are functional as we detect methylation of tyrosine (M2) and phenylalanine (M3). Other modifications are performed by the halogenase, Pep1[18], the methyltransferase, Pep9[18] and oxygenase, Pep10[18] which have previously been characterized through knock out studies in *S.* sp. PKU-MA01144 and *in vitro* feeding experiments. These genes are shared across all three *pcm*/*pep* BGCs. The polyketide/fatty acid sidechain in the pepticinnamin biosynthesis is likely synthesized by eight genes

encoding acyl carrier and/or beta-ketoacyl proteins, a 3-oxoacyl-ACP reductase and a beta-hydroxyacyl-ACP dehydratase based on the protein function predictions, however there is no experimental evidence of which specific genes are involved. Pepticinnamins O and N with a shorter peptide chain are likely shunt products derived from pepticinamin biosynthesis.

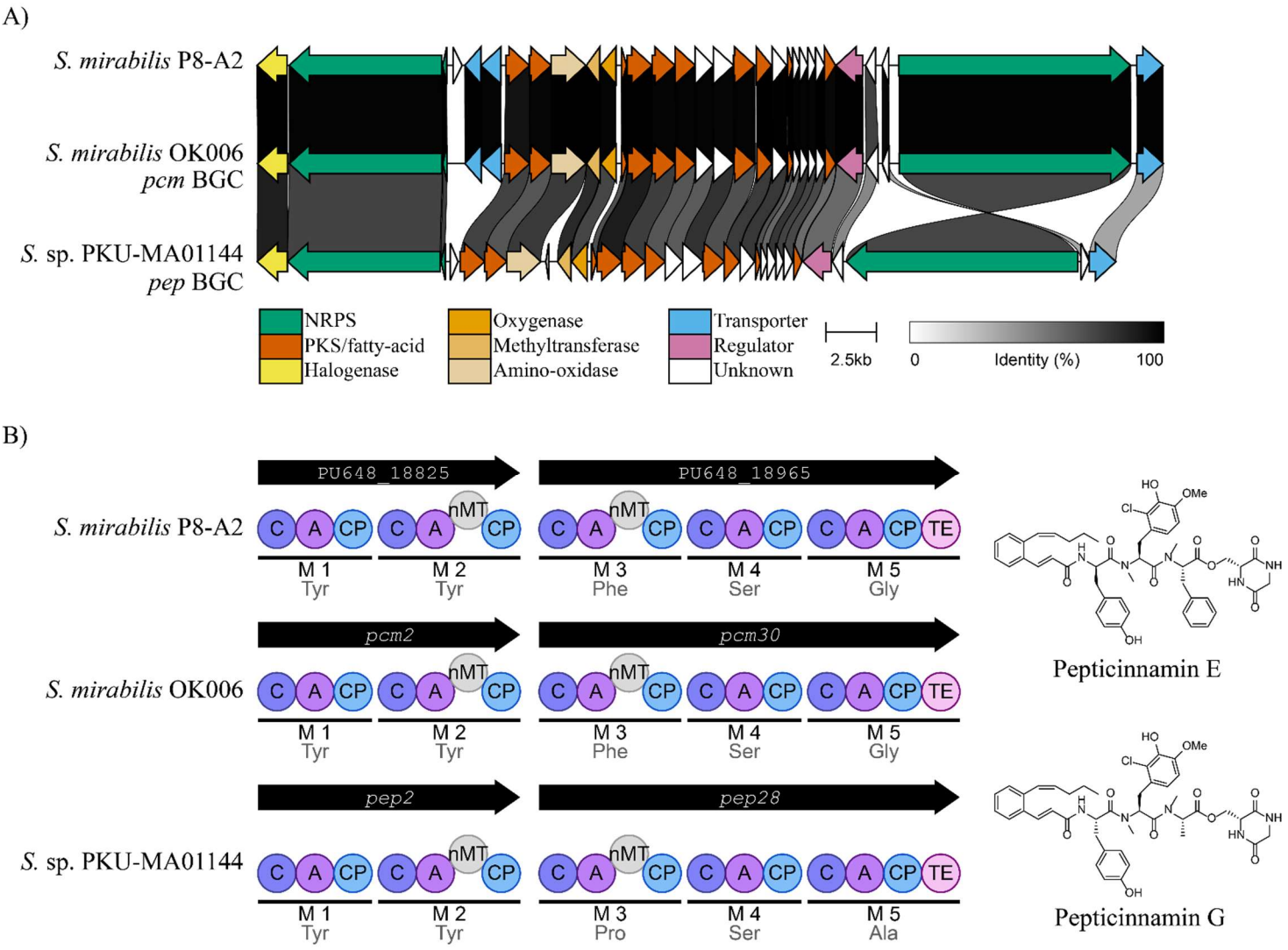

Figure 6. Pepticinnamin biosynthetic gene cluster comparison between three producers. (A) using clinker[31] alignment with gene coloring based on their predicted/elucidated involvement in the biosynthesis. (B) antiSMASH 7.0.[20] overview of the NRPS domains in the three biosynthetic gene clusters. The condensation domains are predicted to link two L-amino acids in all of the BGCs. Pepticinnamin E is produced by *S. mirabilis* P8-A2 and OK006, while pepticinnamin G by *S.* sp. PKU-MA01144.

Experimental section

General Experimental Procedures

Optical rotations were measured on an Autopol III automatic polarimeter (Rudolph Research Analytical, Hackettstown, NJ, USA). IR data were acquired on Bruker Alpha FTIR spectrometer using OPUS version 7.2. The NMR spectra were recorded on a Bruker AVANCE III 800 MHz spectrometer (Bruker, 279 Billerica, MA, USA) equipped with a 5 mm TCI CryoProbe using standard pulse sequences. The ^{1}H and ^{13}C NMR chemical shifts were reported with reference to the residual solvent signals at δ_H 4.87, 3.31 and δ_C 49.1 ppm for CD_3OD. NMR data were processed using MestReNova 12.0. UHPLC- HRMS was performed on an Agilent Infinity 1290 UHPLC (Agilent Technologies, Santa Clara, CA, USA) system equipped with a diode array detector. UV−vis spectra were recorded from 190 to 640 nm. All solvents and chemicals used for HRMS, and chromatography were LC-MS grade, while the solvents for metabolite extraction were of HPLC grade. Water was purified using a Milli-Q system (Millipore, Bedford, MA, USA).

Streptomyces strains and cultivation

S. mirabilis P8-A2[19] and *S. mirabilis* P8-A2 AzdB Q73* (*azdB*^{STOP})[21] were cultured using the international *Streptomyces* project media 2 (ISP2) and Soya Flour Mannitol (MSF) as described by Maleckis et al. 2023.[21] Cultivation was performed in the dark at 30 °C for solid cultures. Pre-culture for large scale inoculations were generated by inoculating baffled flask containing ISP2 liquid medium over night at 30 °C and 180 RPM. The pre-culture was used to inoculate 278 SFM agar plates (5.5 L in total), which were cultured in dark for 10 days at 30°C.

Extraction, isolation, and purification

After 10 days of incubation, the cultured agar was extracted with ethyl acetate (EtOAc) (2 × 2.5L) under ultrasonication for 60 min. The EtOAc phase was thereafter filtered and dried under reduced pressure using a rotary evaporator. The extraction process was repeated again, however this time with 2 × 2.5 L of acidic EtOAc (0.1% v/v formic acid). The EtOAc phase was filtered and dried under reduced pressure to obtain a total of 7.2 g of dried extract.

The crude extract was passed through a pre-packed disposable reverse-phase (C_{18}) 100 g SNAP flash chromatography column (Biotage®, Uppsala, Sweden) and the bound compounds were eluted in a 10 – 100 % acetonitrile (MeCN) (0.1 % FA) – water (0.1 % FA) gradient using a Biotage® Isolera over a period of 1.5 hours with a 45 mL/min flowrate. The collected fractions were subjected to thin-layer chromatography (TLC) on a pre-coated TLC-sheet POLYGRAM® SIL G/UV_{254} (from MACHERY-NAGEL, Germany) 95%-5% (DCM-MeOH) and sprayed with anisaldehyde sulphuric acid.

Pepticinnamin E and its analogues were detected in four fractions (1-4). Fraction 1 was further fractionated using a linear gradient from 50% to 80% MeCN in Milli-Q water over 20 min by an Agilent Infinity 1290 HPLC-DAD (Agilent Technologies) system, with a flow rate of 4 mL/min, UV monitoring at 220, 254, and 282 nm, and a column temperature at 40 °C using a Luna® 5 µm Phenyl-Hexyl 100 Å, LC Column (250 x 10 mm) to yield two subfractions (subfraction 1A and 1B corresponding to pepticinnamin N and O respectively). Fraction 2 was further fractionated using a linear gradient from 65% to 80% MeCN in Milli-Q water over 20 min to yield three subfractions (subfraction 2A, 2B and 2C corresponding to pepticinnamin N, E and O respectively). Fraction 3 was further fractionated using a linear gradient from 60% to 80% MeCN in Milli-Q water over 20 min to yield two subfractions (subfraction 3A and 3B corresponding to pepticinnamin O and P respectively). Fraction 4 was further fractionated using a linear gradient from 60% to 80% MeCN in Milli-Q water over 20 min to yield one subfraction (subfraction 4A corresponding to pepticinnamin P). Subfraction 1A and 2A were mixed to yield pepticinnamin N (**2**, 2 mg). Subfraction 1B and 2B were mixed to yield of pepticinnamin E (**1**, 5 mg). Subfraction 2C and 3A were mixed to yield pepticinnamin O (**3**, 2.5 mg), and finally subfraction 3B and 4A were mixed to yield pepticinnamin P (**4**, 3 mg).

Marfey´s reaction and configuration determination of pepticinnamin E

Compound **1** together with the standards were dissolved in MeOH (2 mg/mL) in a glass vial and dried under nitrogen. Followed by adding 6 N HCl and capping, the vial was heated at 100 °C for 16 h. After cooling to room temperature, the sample was dried under nitrogen. The residue was dissolved in 1 M $NaHCO_3$ and treated with 1% FDAA Marfey reagent (200 µL in acetone solution) and allowed to react at 45 °C for 90 min. After cooling, the samples were quenched with 2 N HCl (20 µL), the reaction mixture was dried under nitrogen, and then dilute with 130 µL MeOH, centrifuged and transferred to 100 µL HPLC vial then analyzed by LC-MS.

The absolute configuration of the non-proteogenic amino acid *N*-methyl-2-chloro-3-hydroxy-4-methoxy-phenylalanine was determined by measuring the optical rotation following the acid hydrolysis where the DOPA derivative was subjected to 6 N HCl and heated at 100 °C for 16 h. Purification from the hydrolyzed mixture was performed by using a linear gradient from 8% to 15% MeCN in Milli-Q water over 20 min by an Agilent Infinity 1290 HPLC-DAD (Agilent Technologies) system. Finally, the specific optical rotation of the isolated compound was recorded.

HPLC and Mass Spectrometry

An ultra-high-performance liquid chromatography-high-resolution mass spectrometry (UHPLC-HRMS) was performed on an Agilent Infinity 1290 UHPLC system equipped with a diode array detector. UV-visible spectra were recorded from 190 to 640 nm. LC/HRMS of 1 µL crude extract and the above-mentioned fraction and

subfractions was performed on a 250 × 2.1 mm i.d., 2.7 μm, Poroshell 120 phenyl-hexyl column (Agilent Technologies) at 60°C using of MeCN and H_2O, both buffered with 20 mM FA, as mobile phases. Initially, a linear gradient of 10% MeCN/H_2O to 100% MeCN over 15 min was employed, followed by isocratic elution of 100% MeCN for 2 min, the gradient was returned to 10% MeCN/H_2O in 0.1 min, and finally isocratic condition of 10% MeCN /H_2O for 2.9 min, all at a flow rate of 0.35 mL/min. MS detection was performed in positive mode on an Agilent 6545 Q-TOF LC/MS equipped with an Agilent Dual Jet Stream electrospray ion source with a drying gas temperature of 250°C, drying gas flow of 8 L/min, sheath gas temperature of 300°C, and sheath gas flow of 12 L/min. Capillary voltage was set to 4000 V and nozzle voltage to 500 V. MS spectra were recorded as centroid data, at an m/z of 100−1700, and MS data processing and analysis were performed using Agilent MassHunter Qualitative Analysis software (Agilent Technologies).

Antimicrobial activity test

For agar diffusion assay,[32] sterile filter paper disks (d = 9 mm) were impregnated with 50 μg of the samples using methanol as the carrier solvent. The impregnated disks were then placed on agar plates previously inoculated with *Staphylococcus aureus* 8325, *Bacillus subtilis* or *Pseudomonas aeruginosa* PAO1. The test sample was considered active when the zone of inhibition was greater than 9 mm. The minimal inhibition concentration values were recorded after incubation at 37°C for 12 hours and 24 hours, for bacteria and fungi, respectively. Protocols for agar diffusion and minimal inhibition concentration were followed by The MIC assay using test strains *Candida albicans* IBT 656 was done by the broth dilution method according to the NCCLS.[33] The test sample was considered active when the MIC values was less than 50 μg/mL.

Cell growth and cytotoxicity assay

Cell growth and cytotoxicity were assessed using the human epithelial prostate cancer cell line LNCaP (RRID:CVCL_0395) and its hormone-refractory derivative C4-2B (RRID:CVCL_4784), as well as two derivative drug-resistant sublines (C4-2B^R and LNCaP^R, respectively) (ref is PMID: 33799432), all of which carry wild-type *RAS* alleles. All cell lines were cultured and maintained in RPMI-1640 medium containing glutaMAX™-I (Gibco, Invitrogen, Carlsbad, CA, United States), supplemented with 10% fetal bovine serum (FBS). Cells were seeded into 6-well plates at 3x10^5 cells/well. After cells attached, the medium in each well was replaced with 2mL of fresh warm medium containing 10μM of the different compounds or vehicle. Cell proliferation dynamics were monitored in real-time using a lens-free Cellwatcher microscopy device (PHIO, Germany). The cell growth curves were generated with the analysis module available from PHIO to determine the total area covered by cells. Cytotoxicity was measured as an endpoint assay of drug-exposure using the CellTox Green Cytotoxicity Assay kit according to

manufacturer's instructions. Briefly, CellTox green cytotoxicity reagent was added to the media at a final concentration of 1X, and the relative cytotoxicity was calculated relative to the control well treated with vehicle.

Pepticinnamin E (**1**) $[\alpha]_D^{29}$ -84.2 (*c* 0.10 MeOH), UV (MeCN/H_2O) λ_{max}: 225 nm and 282 nm. IR (ATR) ν_{max}: 3357, 3248, 2953, 2934, 1744, 1678, 1648, 1637, 1516 1493, 1454, 1326, 1281 and 1204 cm^{-1}. (+)-HRESIMS *m/z*: $[M+H]^+$ Calcd for $C_{49}H_{54}ClN_5O_{10}$ 908.3632; Found 908.3631. ^{1} H NMR and ^{13}CNMR data, Table 1.

Pepticinnamin N (**2**) $[\alpha]_D^{29}$ -84.2 (*c* 0.10 MeOH), UV (MeCN/H_2O) λ_{max}: 223 nm and 282 nm. IR (ATR) ν_{max}: 3267, 3253, 3237, 2951, 2934, 2921, 1730, 1680, 1645, 1634, 1516, 1465, 1434, 1207, 1187, 1136 cm^{-1}. (+)-HRESIMS *m/z*: $[M+H]^+$ Calcd for $C_{49}H_{55}N_5O_{10}$ 874.4022; Found 874.4017. ^{1} H NMR and ^{13}C NMR data, Table 1.

Pepticinnamin O (**3**) $[\alpha]_D^{29}$ -119.2 (*c* 0.10 MeOH), UV (MeCN/H_2O) λ_{max}: 225 nm and 282 nm. IR (ATR) ν_{max}: 2942, 2927, 2912, 1701, 1685, 1676, 1655, 1637,1457, 1439, 1145, 1135, 1042 cm^{-1}. (+)-HRESIMS *m/z*: $[M+H]^+$ Calcd for $C_{44}H_{48}ClN_3O_8$ 782.3203; Found 782.3190. ^{1} H NMR and ^{13}C NMR data, Table 1.

Pepticinnamin P (**4**) $[\alpha]_D^{29}$ -97.2 (*c* 0.10 MeOH), UV (MeCN/H_2O) λ_{max}: 225 nm and 282 nm. IR (ATR) ν_{max}: 2990, 2955, 2918, 2849, 1710, 1684, 1654, 1636, 1509, 1458, 1439, 1267, 1205, 1145, 1136 cm^{-1}. (+)-HRESIMS *m/z*: $[M+H]^+$ Calcd for $C_{44}H_{49}N_3O_8$ 748.3592; Found 748.3596. ^{1}H NMR and ^{13}C NMR data, Table 1.

352 Table 1. ^{1}H (800 MHz) and ^{13}C (200 MHz) NMR Data for Pepticinnamins in CD_3OD

	Pepticinnamin E		Pepticinnamin N		Pepticinnamin O		Pepticinnamin P	
pos.	δ_C, type	δ_H (*J* in Hz)	δ_C, type	δ_H (*J* in Hz)	δ_C, type	δ_H (*J* in Hz)	δ_C, type	δ_H (*J* in Hz)
Cinnamoyl (a)								
1’	165.9, C		167.6, C		167.2, C		167.7, C	
2’	122.5, CH	6.45 (d, 15.7)	122.1, CH	6.48 (d, 15.7)	122.5, CH	6.45 (d, 15.7)	122.1, CH	6.54 (d, 15.7)
3’	140.4, CH	7.77 (d, 15.7)	140.6, CH	7.76 (d, 15.7)	140.4, CH	7.78 (d, 15.7)	140.6, CH	7.75 (d, 15.7)
4’	134.4, C		134.5, C		134.4, C		134.4, C	
5’	127.1, CH	7.66 (d, 7.5)	127.2, CH	7.68 (d, 7.8)	127.0, CH	7.67 (d, 7.6)	127.2, CH	7.67 (d, 7.8)
6’	128.4, CH	7.29 (t, 7.3)	128.3, CH	7.29 (t, 7.2)	128.3, CH	7.28 (m)	128.3, CH	7.29 (td, 1.2, 7.7)
7’	130.4, CH	7.34 (t, 7.4)	130.3, CH	7.34 (m)	130.4, CH	7.33 (td 1.2, 7.3)	130.3, CH	7.31 (td 1.2, 7.5)
8’	131.2, CH	7.22 (d, 7.6)	131.0, CH	7.21 (m)	131.2, CH	7.21 (d, 7.3)	131.1, CH	7.20 (d, 7.5)
9’	139.5, C		139.4, C		139.4, C		139.4, C	
10’	128.2, CH	6.60 (d, 11.4)	128.2, CH	6.59 (d, 11.4)	128.2, CH	6.61 (d, 11.5)	128.2, CH	6.59 (d, 11.4)
11’	135.9, CH	5.86 (dt, 7.4, 11.5)	135.9, CH	5.86 (dt, 7.4, 11.4)	136.0, CH	5.87 (dt, 7.4, 11.5)	135.9, CH	5.85 (dt, 7.5, 11.4)
12’	31.7, CH_2	2.01 (dq, 1.5, 7.3)	31.6, CH_2	2.01 (qd, 1.5, 7.4)	31.6, CH_2	2.01 (qd, 1.5, 7.4)	31.6, CH_2	2.0 (qd, 1.6, 7.4)
13’	23.7, CH_2	1.40 (sext, 7.3)	23.6, CH_2	1.40 (sext, 7.4)	23.7, CH_2	1.39 (sext, 7.4)	23.7, CH_2	1.40 (sext, 7.4)
14’	14.2, CH_3	0.84 (t, 7.3)	14.1, CH_3	0.84 (t, 7.4)	14.2, CH_3	0.83 (t, 7.4)	14.2, CH_3	0.83 (t, 7.4)

Tyrosine (b)								
1	172.6, C		172.4, C		172.5, C		171.2, C	
2	51.5, CH	5.02 (dd, 7.3, 8.0)	51.9, CH	5.01 (m)	51.5, CH	4.99 (t, 7.6)	51.8, CH	5.01 (t, 7.4)
3α	38.4, CH_2	2.62 (dd, 6.9, 13.6)	38.3, CH_2	2.69 (m)	38.4, CH_2	2.6 (dd, 7.0, 13.7)	38.3, CH_2	2.70 (dd, 7.0, 13.5)
3β		2.83 (dd, 8.3, 13.6)		2.89 (m)		2.79 (dd, 8.2, 13.7)		2.91 (dd, 8.2, 13.5)
4	128.8, C		128.7, C		128.7, C		128.8, C	
5/9	131.6, CH	7.04 (d, 8.5)	131.6, CH	7.07 (d, 8.5)	131.5, CH	7.02 (d, 8.5)	131.5, CH	7.06 (d, 8.5)
6/8	116.4, CH	6.73 (d, 8.8)	116.4, CH	6.73 (d, 8.5)	116.4, CH	6.72 (d, 8.5)	116.4, CH	6.73 (d, 8.5)
7	157.5, C		157.4, C		157.5, C		157.5, C	
2-chloro-3-hydroxy-4-methoxy-phenylalanine (c)								
10	31.0, CH_3	2.47 (s)	30.9, CH_3	2.42 (s)	30.7, CH_3	2.42 (s)	30.8, CH_3	2.48 (s)
11	171.9, C		171.6, C		172, C		171.4, C	
12	55.0, CH	5.56 (dd, 4.7, 10.0)	55.8, CH	5.35 (t, 7.4)	54.6, CH	5.62 (dd, 4.6, 10.0)	56.8, CH	5.38 (t, 7.3)
13α	33.2, CH_2	2.76 (dd, 10.0, 14.4)	33.7, CH_2	2.57 (dd, 7.9, 14.1)	33.2, CH_2	2.7 (dd, 10.1, 14.4)	35.2, CH_2	2.56 (dd, 7.0, 13.8)
13β		3.10 (dd, 4.7, 14.4)		2.98 (dd, 7.1, 14.1)		3.09 (dd, 4.6, 14.4)		3.00 (dd, 7.6, 13.8)
14	128.6, C		129.9, C		128.7, C		130.1, C	
15	122.3, CH	6.51 (br. d)	120.6, CH	6.55 (m)	122.1, CH	6.47 (d, 8.3)	120.6, CH	6.57 (dd, 2.1, 8.1)

16	110.3, CH	6.51 (br. d)	111.1, CH	6.66 (dd, 3.3, 8.2)	110.2, CH	6.44 (d, 8.3)	111.2, CH	6.67 (d, 8.6)
17	148.5, C		146.3, C		148.4, C		146.3, C	
18	144.1, C		142.6, C		143.9, C		-	
19	122.1, C		116.3, CH	6.73 (m)	122.0, C		116.2, CH	6.70 (d, 2.1)
-OCH_3	56.5, CH_3	3.57 (s)	54.8, CH_3	3.64 (s)	56.4, CH_3	3.54 (s)	54.9, CH_3	3.67 (s)
N-Me-phenylalanine (d)								
20	33.7, CH_3	2.30 (s)	31.9, CH_3	2.29 (s)	33.4, CH_3	2.32 (s)	32.7, CH3	2.3 (s)
21	171.2, C		169.7, C		172.2, C		170.8, C	
22	60.7, CH	5.22 (dd, 4.6, 11.7)	59.1, CH	5.22 (dt, 4.0, 10.9)	62.1, CH	4.90	62.0, CH	4.95
23α	35.2, CH2	2.94 (dd, 11.8, 14.5)	33.7, CH2	2.88 (m)	35.4, CH_2	2.92 (m)	33.8, CH2	2.91 (dd, 12.3, 14.3)
23β		3.27 (dd, 4.8, 14.5)		3.23 (dd, 4.5, 14.4)		3.34 (dd, 4.0, 14.4)		3.27 (dd, 4.4, 14.4)
24	138.2, C		136.7, C		138.9, C		137.4, C	
25/29	130.2, CH	7.06 (d, 7.1)	128.8, CH	6.96 (d, 8.5)	130.2, CH	7.07 (d, 7.1)	128.8, CH	6.94 (d, 7.1)
26/28	129.7, CH	7.25 (m)	128.3, CH	7.20 (m)	129.7, CH	7.24 (m)	128.2, CH	7.18 (m)
27	128.0, CH	7.22 (m)	126.5, CH	7.20 (m)	127.8, CH	7.21 (d, 7.3)	126.4, CH	7.17 (m)
Serine (e)								
30	167.7, C		166.4, C					
31	55.6, CH	4.28 (t, 3.6)	54.1, CH	4.22 (t, 3.6)				

32α	66.8, CH_2	4.56 (dd, 4.2, 11.3)	65.4, CH2	4.55 (dd, 3.9, 11.4)		
32β		4.41 (dd, 3.3, 11.3)		4.35 (dd, 3.5, 11.4)		
Glycine (e)						
33	168.5, C		167.1, C			
34α	45.5, CH_2	3.92 (dd, 1.0, 17.8)	43.9, CH_2	3.89 (dd, 0.7, 17.7)		
34β		4.04 (dd, 1.0, 17.8)		4.03 (dd, 0.7, 17.7)		

353

ASSOCIATED CONTENT

Supporting Information

LC/HRMS, NMR spectra and ECD curves for compounds **1-4**.

ACKNOWLEDGMENTS

This study was supported by Egyptian governmental scholarship, Danish National Research Foundation (DNRF137) as part of the Center for Microbial Secondary Metabolites (CeMiSt). L.D. acknowledges funding from Carlsberg Infrastructure (CF20-0177). T.W. would furthermore acknowledge funding by the Novo Nordisk Foundation (NNF20CC0035580). Thanks to the support DTU Metabolomics Core; Thanks to the NMR Center at DTU for access to the 800 MHz spectrometer; we would like to thank Kai Blin and Simon Shaw for support with bioinformatic analysis.

References and Notes

(1) Van Keulen, G.; Dyson, P. J. *Adv. Appl. Microbiol.* **2014**, *89*, 217–266.

(2) Ohnishi, Y.; Ishikawa, J.; Hara, H.; Suzuki, H.; Ikenoya, M.; Ikeda, H.; Yamashita, A.; Hattori, M.; Horinouchi, S. *J. Bacteriol.* **2008**, *190*, 4050–4060.

(3) Ikeda, H.; Ishikawa, J.; Hanamoto, A.; Shinose, M.; Kikuchi, H.; Shiba, T.; Sakaki, Y.; Hattori, M.; Omura, S. *Nat. Biotechnol.* **2003**, *21*, 526–531.

(4) Bentley, S. D.; Chater, K. F.; Cerdeño-Tárraga, A. M.; Challis, G. L.; Thomson, N. R.; James, K. D.; Harris, D. E.; Quail, M. A.; Kieser, H.; Harper, D.; Bateman, A.; Brown, S.; Chandra, G.; Chen, C. W.; Collins, M.; Cronin, A.; Fraser, A.; Goble, A.; Hidalgo, J.; Hornsby, T.; Howarth, S.; Huang, C. H.; Kieser, T.; Larke, L.; Murphy, L.; Oliver, K.; O'Neil, S.; Rabbinowitsch, E.; Rajandream, M. A.; Rutherford, K.; Rutter, S.; Seeger, K.; Saunders, D.; Sharp, S.; Squares, R.; Squares, S.; Taylor, K.; Warren, T.; Wietzorrek, A.; Woodward, J.; Barrell, B. G.; Parkhill, J.; Hopwood, D. A. *Nature* **2002**, *417*, 141–147.

(5) Lee, N.; Hwang, S.; Lee, Y.; Cho, S.; Palsson, B.; Cho, B. K. *J. Microbiol. Biotechnol.* **2019**, *29*, 667–686.

(6) Baral, B.; Akhgari, A.; Metsä-Ketelä, M. *Synth. Syst. Biotechnol.* **2018**, *3*, 163–178.

(7) Luo, Y.; Huang, H.; Liang, J.; Wang, M.; Lu, L.; Shao, Z.; Cobb, R. E.; Zhao, H. *Nat. Commun.* **2013**, *4*, 1–8.

(8) Young, T. S.; Walsh, C. T. *Proc. Natl. Acad. Sci.* **2011**, *108*, 13053–13058.

(9) Wakefield, J.; Hassan, H. M.; Jaspars, M.; Ebel, R.; Rateb, M. E. *Front. Microbiol.* **2017**, *8*.

(10) Yang, Z.; Sun, C.; Liu, Z.; Liu, Q.; Zhang, T.; Ju, J.; Ma, J. *J. Nat. Prod.* **2020**, *83*, 1666–1673.

(11) Liu, Q.; Liu, Z.; Sun, C.; Shao, M.; Ma, J.; Wei, X.; Zhang, T.; Li, W.; Ju, J. *Org. Lett.* **2019**, *21*, 2634–2638.

(12) Bae, M.; Kim, H.; Moon, K.; Nam, S. J.; Shin, J.; Oh, K. B.; Oh, D. C. *Org. Lett.* **2015**, *17*, 712–715.

(13) Yu, Z.; Vodanovic-Jankovic, S.; Kron, M.; Shen, B. *Org. Lett.* **2012**, *14*, 4946.

(14) Um, S.; Park, S. H.; Kim, J.; Park, H. J.; Ko, K.; Bang, H. S.; Lee, S. K.; Shin, J.; Oh, D. C. *Org. Lett.* **2015**, *17*, 1272–1275.

(15) Omura, S.; Der Pyl1, V.; Inokoshi, J.; Takahashi, Y.; Takeshima, H. *J. Antibiot.* **1993**, *46*, 222-8.

(16) Toki, S.; Agatsuma, T.; Ochiai, K.; Saitoh, Y.; Ando, K.; Nakanishi, S.; Lokker, N. A.; Giese, N. A.; Matsuda, Y. *J. Antibiot.* **2001**, *54*, 405–414.

(17) Santa Maria, K. C.; Chan, A. N.; O'Neill, E. M.; Li, B. *Chembiochem.* **2019**, *20*, 1387–1393.

(18) Ge, Y.; Wang, G.; Jin, J.; Liu, T.; Ma, X.; Zhang, Z.; Geng, T.; Song, J.; Ma, X.; Zhang, Y.; Yang, D.; Ma, M. *J. Org. Chem.* **2020**, *85*, 8673–8682.

(19) Wibowo, M.; Gotfredsen, C. H.; Sassetti, E.; Melchiorsen, J.; Clausen, M. H.; Gram, L.; Ding, L. *J. Nat. Prod.* **2020**, *83*, 3519–3525.

(20) Blin, K.; Shaw, S.; Augustijn, H. E.; Reitz, Z. L.; Biermann, F.; Alanjary, M.; Fetter, A.; Terlouw, B. R.; Metcalf, W. W.; Helfrich, E. J. N.; Van Wezel, G. P.; Medema, M. H.; Weber, T. *Nucleic Acids Res.* **2023**, *51*, W46–W50.

(21) Maleckis, M.; Wibowo, M.; Gren, T.; Jarmusch, S. A.; Sterndorff, E. B.; Booth, T.; Henriksen, N. N. S. E.; Whitford, C. M.; Jiang, X.; Jørgensen, T. S.; Ding, L.; Weber, T. *bioRxiv* **2023**.

(22) Goodman, J. *J. Chem. Inf. Model.* **2009**, *49*, 2897–2898.

(23) Van Santen, J. A.; Kautsar, S. A.; Medema, M. H.; Linington, R. G. *Nat. Prod. Rep.* **2021**, *38*, 264–278.

(24) Hinterding, K.; Hagenbuch, P.; Re, J.; Waldmann, H. *Angew. Chem.* **1998**, *37*, 1236-1239.

(25) Tan, K.-T.; Guiu-Rozas, E.; Bon, R. S.; Guo, Z.; Delon, C.; Wetzel, S.; Arndt, S.; Alexandrov, K.; Waldmann, H.; Goody, R. S.; Wu, Y.-W.; Blankenfeldt, W. *J. Med. Chem.* **2009**, *52*, 8025–8037.

(26) Thutewohl, M.; Kissau, L.; Popkirova, B.; Karaguni, I.-M.; Nowak, T.; Bate, M.; Kuhlmann, J.; Müller, O.; Waldmann, H. *Bioorg. Med. Chem.* **2003**, *11*, 2617–2626.

418 (27) Dai, X.; Sun, Y.; Zhang, T.; Ming, Y.; Hongwei, G. *J. Enzyme. Inhib. Med. Chem.* **2020**, *35*,
419 1027–1044.

420 (28) Thutewohl, M.; Waldmann, H. *Bioorg. Med. Chem.* **2003**, *11*, 2591–2615.

421 (29) Sebti, S. M.; Der, C. J. *Nat. Rev. Cancer.* **2003**, *3*, 945–951.

422 (30) Shiomi, K.; Yang, H.; Inokoshi, J.; Van Der Pyl, D.; Nakagawa, A.; Takeshima, H.; Omura, S.
423 *J. Antibiot.* **1993**, *46*, 229–234.

424 (31) Gilchrist, C. L. M.; Chooi, Y. *Bioinform.* **2021**, *37*, 2473–2475.

425 (32) Bauer, A. W.; Kirby, W. M.; Sherris, J. C.; Turck, M. Am. J. Clin. Pathol. **1966**, *45*, 493-496.

426 (33) Standard, C. L. S. I. M27; Reference Method for Broth Dilution Antifungal Susceptibility
427 Testing of Yeasts. **2017**.